Steel and Composite Structures, *Vol. 32, No. 5 (2019) 595-610*
DOI: https://doi.org/10.12989/scs.2019.32.5.595

Static and dynamic behavior of (FG-CNT) reinforced porous sandwich plate using energy principle

Mohammed Medani [1,2], Abdelillah Benahmed [1,2], Mohamed Zidour[*3,4], Houari Heireche [1,2], Abdelouahed Tounsi [5,6], Abdelmoumen Anis Bousahla [2,7], Abdeldjebbar Tounsi [5] and S.R. Mahmoud [8]

[1] *University Djillali Liabes- Sidi-Bel-Abbès, BP 89, Sidi Bel Abbès 22000, Algeria*
[2] *Laboratory of Modeling and Multi-Scale Simulation, Department of Physics, Faculty of Exact Science University of Sidi Bel Abbes, Algeria*
[3] *University Ibn Khaldoun, BP 78 Zaaroura, 14000 Tiaret, Algeria*
[4] *Laboratory of Geomatics and Sustainable Development, University of Ibn Khaldoun-Tiaret, Algeria*
[5] *Laboratory of Materials and Hydrology, University of Sidi Bel Abbes, BP 89 Ben M'hidi, 22000 Sidi Bel Abbes, Algeria*
[6] *Department of Civil and Environmental Engineering, King Fahd University of Petroleum & Minerals, 31261 Dhahran, Eastern Province, Saudi Arabia*
[7] *Centre Universitaire Ahmed Zabana de Relizane, Algérie*
[8] *GRC Department, Jeddah Community College, King Abdulaziz University, Jeddah 21589, Saudi Arabia*

(*Received March 13, 2019, Revised August 3, 2019, Accepted August 13, 2019*)

Abstract. This paper deals with the static and dynamic behavior of Functionally Graded Carbon Nanotubes (FG-CNT)-reinforced porous sandwich (PMPV) polymer plate. The model of nanocomposite plate is investigated within the first order shear deformation theory (FSDT). Two types of porous sandwich plates are supposed (sandwich with face sheets reinforced / homogeneous core and sandwich with homogeneous face sheets / reinforced core). Functionally graded Carbon Nanotubes (FG-CNT) and uniformly Carbon Nanotubes (UD-CNT) distributions of face sheets or core porous plates with uniaxially aligned single-walled carbon nanotubes are considered. The governing equations are derived by using Hamilton's principle. The solution for bending and vibration of such type's porous plates are obtained. The detailed mathematical derivations are provided and the solutions are compared to some cases in the literature. The effect of the several parameters of reinforced sandwich porous plates such as aspect ratios, volume fraction, types of reinforcement, number of modes and thickness of plate on the bending and vibration analyses are studied and discussed. On the question of porosity, this study found that there is a great influence of their variation on the static and vibration of porous sandwich plate.

Keywords: nanotubes; FG-CNTRC; bending; shear deformation; nanocomposite; porosities; sandwich

1. Introduction

A new class of composites that called functionally graded materials (FGMs) has a great practical importance, because of their vast applications in many industrial and engineering fields (Avcar and Alwan 2017, Bouazza *et al*. 2015, Rezaiee-Pajand *et al*. 2019, Ahouel *et al*. 2016, Attia *et al*. 2018, Beldjelili *et al*. 2016, Bellifa *et al*. 2017a, Boulefrakh *et al*. 2019, Bounouara *et al*. 2016, Bourada *et al*. 2018, Bousahla *et al*. 2016, Chaabane *et al*. 2019, Fourn *et al*. 2018, Khetir *et al*. 2017, Zemri *et al*. 2015, Tlidji *et al*. 2019). Recently, Avcar (2019) analyzed the free vibration of imperfect sigmoid and power law functionally graded beams. a variety of theoretical study analyzed a new quasi-3D shear deformation theory for functionally graded plates and beams (Abualnour *et al*. 2018, Benchohra *et al*. 2018, Boukhlif *et al*. 2019, Boutaleb *et al*. 2019, Draiche *et al*. 2016, Karami *et al*. 2018b, Younsi *et al*. 2018, Zaoui *et al*. 2019). The Functionally Graded Carbon Nanotubes (FG-CNT)- reinforced material is formed by varying the distribution of carbon nanotubes (CNTs) reinforcement microstructurally in the matrix composites. The (FG-CNTRC) material leads to a new structure which can resist a large mechanical loadings (Hajmohammad *et al*. 2018). Nowdays, many studies indicated that the (CNTs) have an excellent candidate for the reinforcement of polymer nano-composites due to their high elastic modulus, marvelous mechanical, electrical, thermal properties, tensile strength and low density (Iijima 1991, Bensattalah *et al*. 2016, 2018a, b, 2019, Chemi *et al*. 2015, Rakrak *et al*. 2016, Chemi *et al*. 2018, Hamidi *et al*. 2018, Mehar *et al*. 2019b, Dresselhaus and Avouris 2001, Kolahchi *et al*. 2015, Mehar *et al*. 2017d, Zidour *et al*. 2015, Mehar and Panda 2016a, Semmah *et al*. 2019, Belmahi *et al*. 2018, Hamza-Cherif *et al*. 2018, Dihaj *et al*. 2018, Belmahi *et al*. 2019). (Asadi and Wang 2017) studied the dynamic stability analysis of a pressurized FG-CNTRC cylindrical shell interacting with supersonic airflow. Ajayan *et al*. (1994) investigated the composites (CNTRCs) that are made from polymer reinforced by aligned carbon nanotube. A short time ago, the application of (FG-CNTRC) material is growing rapidly in engineering domain, due to excellent properties (Muller *et al*. 2003). Therefore, varieties of theoretical, computer

*Corresponding author, Ph.D.,
E-mail: zidour.m@univ-tiaret.dz

ISSN: 1229-9367 (Print), 1598-6233 (Online)

and experimental simulation approaches used carbon nanotubes (CNTs) for reinforcing nano-composite structures, due to its importance (Mehar and Panda 2016b, Bakhadda *et al*. 2018, Mehar *et al*. 2017a, Mehar and Panda 2017b, 2018e). Recently researchers have developed elasticity solutions, they indicate that the carbon nanotubes (CNTs) can be used in nanocomposite structures (Asadi and Wang 2017, Lakshmipathi and Vasudevan 2019), free vibration and buckling responses of functionally graded carbon nanotube-reinforced composite are studied by (Moradi-Dastjerdi 2016, Mehar and Panda 2017a, Shafiei and Setoodeh 2017), embedded FGSWCNT-reinforced micro and nano-plates (Kolahchi *et al*. 2015, Mehar *et al*. 2018a). Damping and vibration of viscoelastic curved microbeam reinforced with FG-CNTs resting on viscoelastic medium using strain gradient theory and DQM are analyzed by Allahkarami *et al*. (2017). Varieties of experimental, theoretical, and computer simulation approaches used functionally graded and reinforced polymer (Mehar and Panda 2016c, 2018c, Baseri *et al*. 2016, Kar and Panda 2015, Mehar *et al*. 2017b, Panda *et al*. 2012).

However, the manufacturing processes of (FG-CNT)-reinforced nanocomposites are complex and can lead to the appearance of porosity, which affect the mechanical properties of the structure. The presence of small cavities in the structure named pores, which contains gaseous matter, this defect is due to improper air extraction due to various parameters such as viscosity of the matrix, vacuum pressure or humidity when storing the material. Nonlinear bending of functionally graded porous micro/nano-beams reinforced with graphene platelets based upon nonlocal strain gradient theory (Sahmani *et al*. 2018). Costa *et al*. (2001) analyzed the influence of porosity on the ILSS of carbon/epoxy and carbon/bismaleimide fabric laminates. Chen *et al*. (2017) also gave the discussion on nonlinear vibration and postbuckling of functionally graded graphene reinforced porous nanocomposite beams. Sahmani *et al*. (2018) investigated the nonlinear axial instability of functionally graded porous micro/nano-plates reinforced with graphene platelets using unified nonlocal strain gradient plate model. In another study, found the effect of porosity on mechanical response of functionally graded beams with and without elastic foundations (Kováčik 1999, Ait Yahia *et al*. 2015, Ait Atmane *et al*. 2017, Bourada *et al*. 2019, Benahmed *et al*. 2019).

The limits of presence of porosity in composite parts is fixed according to the applications: a rate of porosities exceeding 1% is not tolerable in the aerospace structures (Liu *et al*. 2006); unlike other applications where a level of 5% or more can be tolerated (Ghiorse 1993). In the present analysis for fully isolated pores of nearly spherical or elliptical shape, the rate of porosities doesn't exceeded 4%. In the same way, Ait Yahia *et al*. (2015) investigated the wave propagation of an infinite FG-plate having porosities by using various simple higher-order shear deformation theories. In another hand, a variety theoretical study analyzed variety structures with porosity (Karami *et al*. 2018a, Guessas *et al*. 2018, Benahmed *et al*. 2019, Shahsavari *et al*. 2018).

The principal advantage of composite sandwich idea is that the resulting structural element has lofty bending stiffness and strength to weight ratio. Their low self-weight is considered a remarkable advantage compared with traditional structures. Composite sandwiches are constituted by two skins and thick core, which can be used for plate or slab type structural applications. The nanocomposite sandwiches composed of two phases which are (CNT) as dispersed phase and polymer as the matrix. The contact model was later extended by Hu and Hwu (1995) for sandwich beams by including the effects of transverse shear deformations and rotary inertia, and by Shu and Fan (1996) for bi-material beams. The use of sandwich structures is growing very rapidly all over the world and has received increasing attention due to their superior characteristics. Shokravi (2017) investigated the buckling of sandwich plates with (FG-CNT)-reinforced layers resting on orthotropic elastic medium using Reddy plate theory. Alankaya and Erdonmez (2017) presented the bending performance of laminated sandwich shells in hyperbolic paraboloidal form. Li *et al*. (2019) presented the mechanical Properties of L-joint with composite sandwich structure. Xiao *et al*. (2018) presented the effect of face-sheet materials on the flexural behavior of aluminum foam sandwich. Sharma *et al*. (2018) proposed a higher-order finite-boundary element model for vibroacoustic responses of laminated composite sandwich structure. Safaei *et al*. (2019) investigated the Frequency-dependent forced vibration analysis of nanocomposite sandwich plate under thermo-mechanical loads. In recent years, many paper studied the mechanical behavior of sandwich such as: Static analysis (Dash *et al*. 2018, 2019, Mahapatra *et al*. 2017a, Mehar *et al*. 2018c, d, Mehar and Panda 2018d, 2019), bending and buckling analysis (Katariya *et al*. 2017, Mehar *et al*. 2019a) and vibrational behaviors (Mehar and Panda 2018a, Mehar et al. 2016, 2017c, 2018b, Meksi *et al*. 2019, Mehar and Panda 2018b). Many other papers studied the sandwich structures (Abdelaziz *et al*. 2017, Belabed *et al*. 2018, Draoui *et al*. 2019, El-Haina *et al*. 2017, Zarga *et al*. 2019, Menasria *et al*. 2017).

The material properties of Functionally Graded Carbon Nanotube reinforced composite (FG-CNTRC) are supposed to vary continuously in the thickness direction. They are estimated through the rule of mixture. The superlative properties of carbon nanotubes, make it an excellent reinforcement for polymer matrix and have shown increasing attention in the past years. Consequently, Lei *et al*. (2013) integrated the buckling of Functionally Graded Carbon Nanotube reinforced composite (FG-CNTRC)-plates using the element-free (kp-Ritz) method. Mehar and Panda (2017b) evaluated the thermoelastic of FG-CNT reinforced shear deformable composite plate under various loading.

Due to difficulties encountered in experimental methods and molecular dynamics (MD) simulations, the continuum mechanics methods are often used to investigate the behaviour of various structures (Avcar 2015, Belkacem *et al*. 2018, Bellifa *et al*. 2017b, Bouadi *et al*. 2018, Bouhadra *et al*. 2018, Cherif *et al*. 2018, Chikh *et al*. 2017, Kaci *et al*. 2018, Kadari *et al*. 2018, Mokhtar *et al*. 2018, Mouffoki *et*

al. 2017, Yazid *et al*. 2018, Youcef *et al*. 2018, Zine *et al*. 2018, Baltacioglu and Civalek 2018). In most applications, elastic foundation presented by Winkler and Pasternak are widely used. They were introducing the second parameter to take into account the existence of shear stress. Avcar and Mohammed (2018) studied the free vibration of functionally graded beams resting on Winkler-Pasternak foundation. The nonlinear vibration analysis of laminated plates resting on nonlinear two-parameters elastic are analyzed by Akgoz and Civalek (2011). Avcar (2016) investigated the effects of material non-homogeneity and two parameters elastic foundations on fundamental frequency parameters of Timoshenko beams.

The present paper focuses on the development of a model to investigate the static and vibration problems of (CNTRC)-plates with porosity reinforced by CNTs using the shear deformation plate theory. The Hamilton's principle in conjunction with Eringen nonlocal elasticity and surface elasticity theories are used to obtain governing Equations. The simply supported (CNTRC) sandwich plates with porosity are considered and the influences of various parameters on the deflections, stresses and natural frequencies of such sandwich plates with porosity with (face sheet reinforced/homogeneous core and homogeneous face sheet/reinforced core) are presented and discussed in relation to several important aspects such as plate thickness, aspect ratios, volume fraction of (CNTs) and sandwich plate with porosity types, etc. Comparisons of obtained analytical solutions with results from the existing literature are provided.

2. Geometrical configuration and material properties of sandwich reinforced porous plate

Consider an (FG-CNTRC) sandwich porous plate with length (a), width (b) and uniform thickness (h) as shown in Figs. 1 and 2. The sandwich porous plate composed of three layers referring in (x, y, z) coordinates system. The top and bottom faces of the sandwich plate with porosity are at z = ±h/2. In this investigation, the sandwich porous plate is constituted of three elastic layers, from bottom to top of the plate are namely by h1 = -h/2, h2, h3, h4 = h/2, respectively.

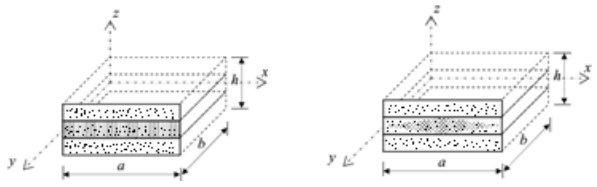

(a) UD-CNT (b) FG-CNT

Fig. 1 Geometries of core reinforced sandwich porous plates

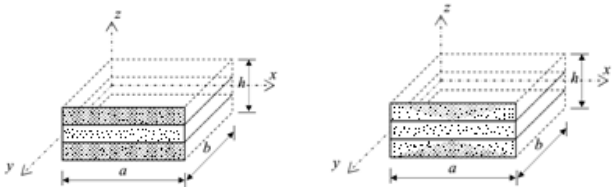

(a) UD-CNT (b) FG-CNT

Fig. 2 Geometries of top and bottom face sheets reinforced sandwich porous plates

The uniform distribution (UD) and functionally graded distribution (FG) of (CNTs) are proposed to reinforce the face sheets or core layers of porous plates. The volume fraction of (CNTs) within the area varies through the thickness of the layers.

The (CNTRC)-porous plate is made of a mixture of uniaxially aligned single-walled carbon nanotubes (CNTs) and anisotropic polymer matrix. According to the rule of mixture model employed to estimate the effective material properties of (CNTRC)-porous plate, the effective Young's modulus and shear modulus of (CNTRC) porous plate can be expressed as Zhu *et al*. (2012)

$$E_{11} = \eta_1 V_{cnt} E_{11}^{cnt} + V_p E^p \tag{1a}$$

$$\frac{\eta_2}{E_{22}} = \frac{V_{cnt}}{E_{22}^{cnt}} + \frac{V_p}{E^p} \tag{1b}$$

$$\frac{\eta_3}{G_{12}} = \frac{V_{cnt}}{G_{12}^{cnt}} + \frac{V_p}{G^p} \tag{1c}$$

where $E_{11}^{cnt}, E_{22}^{cnt}$, E^P and G_{12}^{cnt}, G^P are Young's moduli and shear modulus of SWCNTs and polymer matrix respectively. The (CNT) efficiency parameters (η_1, η_2, η_3) associated with the volume fraction (V_{cnt}) used in the present paper can be defined as (Zhu *et al*. 2012):

η_1 = 0.149 and $\eta_2 = \eta_3$ = 0.934 for the case of V_{cnt}^* = 0.11
η_1 = 0.150 and $\eta_2 = \eta_3$ = 0.941 for the case of V_{cnt}^* = 0.14
η_1 = 0.149 and $\eta_2 = \eta_3$ = 1.381 for the case of V_{cnt}^* = 0.17

The Young's modulus of the polymer matrix, under porosity, which may be a function of porosity change, are defined by (Kováčik 1999)

$$E_p = E_p^0 \left(1 - p / p_0\right) \tag{2}$$

Where E^P is the effective Young's modulus of the reinforced porous matrix, p is the porosity, E_0^P is Young's modulus of the matrix without porosity, p_0 represent the porosity at which the effective Young's modulus becomes zero.

Others properties in terms of mass density ρ and Poisson's ratio (ν) these can be defined as

$$\begin{aligned} \nu_{12} &= V_{cnt} \nu_{12}^{cnt} + V_p \nu^p, \\ \rho &= V_{cnt} \rho^{cnt} + V_p \rho^p \end{aligned} \tag{3a}$$

Where ν_{cnt} and ν_p are the volume fractions of the (CNT)

and porous matrix respectively. The mass density is may also be a function of porosity change.

$$\rho_p = \rho_p^0\left(1-\rho/\rho_0\right) \tag{3b}$$

The volume fraction of two sandwich plate is assumed to obey a function used for describing the distributions of aligned (CNT) along the thickness direction of sandwich plates depicted in Figs. 1 and 2:

For core reinforced sandwich plate

$$\text{core UD-CNT} \begin{cases} V^{(1)} = 0 \\ V^{(2)} = V_{cnt}^{*} \\ V^{(3)} = 0 \end{cases}$$

$$\text{core FG-CNT} \begin{cases} V^{(1)} = 0 \\ V^{(2)} = 2\left(\dfrac{|z|}{h_2}+1\right)V_{cnt}^{*} \\ V^{(3)} = 0 \end{cases} \tag{4}$$

For top and bottom face sheets reinforced sandwich plate

$$\text{Face sheets UD-CNT} \begin{cases} V^{(1)} = V_{cnt}^{*} \\ V^{(2)} = 0 \\ V^{(3)} = V_{cnt}^{*} \end{cases}$$

$$\text{Face sheets FG-CNT} \begin{cases} V^{(1)} = 2\left(\dfrac{h_2-|z|}{h_2-h_1}\right)V_{cnt}^{*} \\ V^{(2)} = 0 \\ V^{(3)} = 2\left(\dfrac{|z|-h_3}{h_4-h_3}\right)V_{cnt}^{*} \end{cases} \tag{5}$$

Where V_{cnt}^{*} is the given volume fraction of (CNTs), which can be obtained from the following equation

$$V_{cnt}^{*} = \frac{W_{cnt}}{W_{cnt}+(\rho^{cnt}/\rho^{m})(1-W_{cnt})} \tag{6}$$

where W_{cnt} is the mass fraction of the carbon nanotube in the nano-composite plate.

3. Theoretical formulation

For Carbon Nanotube reinforced composite (CNTRC)-sandwich plates, the equations of motion used The displacement field can be expressed using the first order shear deformation plate theory (FSDT).

$$\begin{cases} u\left(x,y,z,t\right) = u_0\left(x,y,t\right)+z\,\varphi_x \\ v\left(x,y,z,t\right) = v_0\left(x,y,t\right)+z\,\varphi_y \\ w\left(x,y,t\right) = w_0\left(x,y,t\right) \end{cases} \tag{7}$$

In which u_0, v_0, and w_0 are the mid-plane axial displacement displacements along the x, y and z directions, t is time and φ_x, φ_y are the total bending rotation of the cross-section at any point of the reference plane.

The linear in-plane and transverse shear strains are given by

$$\begin{cases} \varepsilon_{xx} = \dfrac{\partial u_0}{\partial x}+z\,\dfrac{\partial \varphi_x}{\partial x} \\ \varepsilon_{yy} = \dfrac{\partial v_0}{\partial y}+z\,\dfrac{\partial \varphi_y}{\partial y} \\ \gamma_{xy} = \dfrac{\partial u_0}{\partial y}+\dfrac{\partial v_0}{\partial x}+z\left(\dfrac{\partial \varphi_x}{\partial y}+\dfrac{\partial \varphi_y}{\partial x}\right) \end{cases} \tag{8a}$$

$$\begin{cases} \gamma_{xz} = \varphi_x+\dfrac{\partial w_0}{\partial x} \\ \gamma_{yz} = \varphi_y+\dfrac{\partial w_0}{\partial y} \end{cases} \tag{8b}$$

The expression of the constitutive relations is written in the form

$$\begin{Bmatrix} \sigma_{xx} \\ \sigma_{yy} \\ \sigma_{yz} \\ \sigma_{xz} \\ \sigma_{xy} \end{Bmatrix} = \begin{bmatrix} Q_{11} & Q_{12} & 0 & 0 & 0 \\ Q_{12} & Q_{22} & 0 & 0 & 0 \\ 0 & 0 & Q_{44} & 0 & 0 \\ 0 & 0 & 0 & Q_{55} & 0 \\ 0 & 0 & 0 & 0 & Q_{66} \end{bmatrix} \begin{Bmatrix} \varepsilon_{xx} \\ \varepsilon_{yy} \\ \varepsilon_{yz} \\ \gamma_{xz} \\ \gamma_{xy} \end{Bmatrix} \tag{9}$$

Where Q_{ij} are the transformed elastic constants

$$Q_{11} = \frac{E_{11}}{1-\upsilon_{12}\upsilon_{21}}, \quad Q_{22} = \frac{E_{22}}{1-\upsilon_{12}\upsilon_{21}}, \quad Q_{12} = \frac{\upsilon_{21}E_{11}}{1-\upsilon_{12}\upsilon_{21}} \tag{10a}$$

$$Q_{66} = G_{12}, \quad Q_{55} = G_{13}, \quad Q_{44} = G_{23} \tag{10b}$$

The Hamilton's principle is applied to produce the equations of motion.

$$\int_0^t \left(\delta U+\delta V+\delta K\right)dt = 0 \tag{11}$$

Where δU, δV, and δK are the virtual variation of the strain energy, the virtual work done by external forces and the virtual kinetic energy.

The expression of the linear stain energy is

$$\delta U = \sum_{n=1}^{3}\int_{h_n}^{h_{n+1}}\int_A \sigma_{xx}\delta\varepsilon_{xx}+\sigma_{yy}\delta\varepsilon_{yy}+\sigma_{xy}\delta\gamma_{xy}+\sigma_{yz}\delta\gamma_{yz}+\sigma_{xz}\delta\gamma_{xz}\,dA\,dx \tag{12}$$

By substituting Eq. (8) into Eq. (12), one obtains

$$\delta U = \int_A \{ N_{xx}\delta u_{0,x} - M_{xx}\delta\varphi_{x,x} + Q_{xz}\delta(\varphi_x + w_{0,x}) + N_{yy}\delta v_{0,y} + M_{yy}\delta\varphi_{y,y} + Q_{yz}\delta(\varphi_y + w_{0,y}) + N_{xy}(\delta u_{0,y} + \delta v_{0,x}) + M_{xy}\delta(\varphi_{x,y} + \varphi_{y,x}) \} dxdy \quad (13)$$

In which N is the axial force, M is the bending moment and Q is the shear force. The stress resultants used in Eq. (13) are defined as

$$(N_{xx}, N_{yy}, N_{xy}) = \sum_{n=1}^{3} \int_{h_n}^{h_{n+1}} (\sigma_{xx}, \sigma_{yy}, \sigma_{xy}) dz \quad (14a)$$

$$(M_{xx}, M_{yy}, M_{xy}) = \sum_{n=1}^{3} \int_{h_n}^{h_{n+1}} z(\sigma_{xx}, \sigma_{yy}, \sigma_{xy}) dz \quad (14b)$$

$$(Q_{xz}, Q_{yz}) = \sum_{n=1}^{3} \int_{h_n}^{h_{n+1}} (\sigma_{xz}, \sigma_{yz}) dz \quad (14c)$$

By substituting Eqs. (8) and (9) into Eq. (14), one obtains the stress resultants in the form of material stiffness and displacement components.

$$\begin{Bmatrix} N_{xx} \\ N_{yy} \\ N_{xy} \end{Bmatrix} = \begin{bmatrix} A_{11} & A_{12} & 0 \\ A_{12} & A_{22} & 0 \\ 0 & 0 & A_{66} \end{bmatrix} \begin{Bmatrix} \frac{\partial u_0}{\partial x} \\ \frac{\partial v_0}{\partial y} \\ \frac{\partial u_0}{\partial y} + \frac{\partial v_0}{\partial x} \end{Bmatrix} + \begin{bmatrix} B_{11} & B_{12} & 0 \\ B_{12} & B_{22} & 0 \\ 0 & 0 & B_{66} \end{bmatrix} \begin{Bmatrix} \frac{\partial \phi_x}{\partial x} \\ \frac{\partial \phi_y}{\partial y} \\ \left(\frac{\partial \phi_x}{\partial y} + \frac{\partial \phi_y}{\partial x}\right) \end{Bmatrix} \quad (15a)$$

$$\begin{Bmatrix} M_{xx} \\ M_{yy} \\ M_{xy} \end{Bmatrix} = \begin{bmatrix} B_{11} & B_{12} & 0 \\ B_{12} & B_{22} & 0 \\ 0 & 0 & B_{66} \end{bmatrix} \begin{Bmatrix} \frac{\partial u_0}{\partial x} \\ \frac{\partial v_0}{\partial y} \\ \frac{\partial u_0}{\partial y} + \frac{\partial v_0}{\partial x} \end{Bmatrix} + \begin{bmatrix} C_{11} & C_{12} & 0 \\ C_{12} & C_{22} & 0 \\ 0 & 0 & C_{66} \end{bmatrix} \begin{Bmatrix} \frac{\partial \phi_x}{\partial x} \\ \frac{\partial \phi_y}{\partial y} \\ \left(\frac{\partial \phi_x}{\partial y} + \frac{\partial \phi_y}{\partial x}\right) \end{Bmatrix} \quad (15b)$$

$$\begin{Bmatrix} Q_{yz} \\ Q_{xz} \end{Bmatrix} = \begin{bmatrix} D_{44} & 0 \\ 0 & D_{55} \end{bmatrix} \begin{Bmatrix} \varphi_y + \frac{\partial w_0}{\partial y} \\ \varphi_x + \frac{\partial w_0}{\partial x} \end{Bmatrix} \quad (15c)$$

Where A_{ij}, B_{ij}, C_{ij}, D_{ij}, are the plate stiffness coefficients, defined by

$$[A_{ij}, B_{ij}, C_{ij}] = \sum_{n=1}^{3} \int_{h_n}^{h_{n+1}} Q_{ij}[1, z, z^2] dz; \quad i, j = 1,2,6 \quad (16a)$$

$$[D_{ij}] = \sum_{n=1}^{3} \beta \int_{h_n}^{h_{n+1}} Q_{ij} dz; \quad i, j = 4,5 \quad (16b)$$

Where β = 5/6 is the correction factor of the shear deformation depending on the shape of the cross-section.

For the (CNTRC) plates under bending loading q, the virtual work done by external loadings is

$$\delta V = -\int_A q\delta w_0 dxdy \quad (17)$$

The virtual kinetic energy of the system can be expressed as follows

$$\begin{aligned} \delta K &= \int_V \rho(z)[\dot{u}\delta\dot{u} + \dot{v}\delta\dot{v} + \dot{w}\delta\dot{w}] dxdydz \\ &= \int_V \{ I_0(\dot{u}_0\delta\dot{u}_0 + \dot{v}_0\delta\dot{v}_0 + \dot{w}_0\delta\dot{w}_0) + \\ &I_1(\dot{u}_0\delta\dot{\varphi}_x + \dot{v}_0\delta\dot{\varphi}_y + \dot{\varphi}_x\delta\dot{u}_0 + \dot{\varphi}_y\delta\dot{v}_0) + \\ &I_2(\dot{\varphi}_x\delta\dot{\varphi}_x + \dot{\varphi}_y\delta\dot{\varphi}_y) \} dxdy \end{aligned} \quad (18a)$$

Where (I_0, I_1, I_2) are the mass moment of inertias, defined as follows

$$[I_0, I_1, I_2] = \sum_{n=1}^{3} \int_{h_n}^{h_{n+1}} \rho(z)[1, z, z^2,] dz \quad (18b)$$

By substituting Eqs. (13), (17) and (18) into Eq. (11), Then, integrating by parts and collecting the coefficients of δu_0, δv_0, δw_0, $\delta\varphi_x$ and $\delta\varphi_y$, the following Euler-Lagrange equation can be obtained.

$$\delta u_0 = 0 \quad or \quad \frac{\partial N_{xx}}{\partial x} + \frac{\partial N_{xy}}{\partial y} = I_0\ddot{u}_0 + I_1\ddot{\varphi}_x \quad (19a)$$

$$\delta v_0 = 0 \quad or \quad \frac{\partial N_{yy}}{\partial y} + \frac{\partial N_{xy}}{\partial x} = I_0\ddot{v}_0 + I_1\ddot{\varphi}_y \quad (19b)$$

$$\delta w_0 = 0 \quad or \quad \frac{\partial P_{xz}}{\partial x} + \frac{\partial P_{yz}}{\partial y} + q = I_0\ddot{w}_0 \quad (19c)$$

$$\delta\varphi_x = 0 \quad or \quad \frac{\partial M_{xx}}{\partial x} - P_{xz} + \frac{\partial M_{xy}}{\partial y} = I_1\ddot{u}_0 + I_2\ddot{\varphi}_x \quad (19d)$$

$$\delta\varphi_y = 0 \quad or \quad \frac{\partial M_{yy}}{\partial y} - P_{yz} + \frac{\partial M_{xy}}{\partial x} = I_1\ddot{v}_0 + I_2\ddot{\varphi}_y \quad (19e)$$

Under the following boundary conditions of (CNTRC) plates, the following Navier solution form for the displacement functions expanded in double trigonometric series that satisfies the boundary conditions

$$\begin{aligned}
u_0(x,y,t) &= \sum_{M=1}^{\infty}\sum_{N=1}^{\infty} U_{MN}\, e^{i\omega t}\cos(\alpha x)\sin(\zeta y)\\
v_0(x,y,t) &= \sum_{M=1}^{\infty}\sum_{N=1}^{\infty} V_{MN}\, e^{i\omega t}\sin(\alpha x)\cos(\zeta y)\\
w_0(x,y,t) &= \sum_{M=1}^{\infty}\sum_{N=1}^{\infty} W_{MN}\, e^{i\omega t}\sin(\alpha x)\sin(\zeta y)\\
\phi_x(x,y,t) &= \sum_{M=1}^{\infty}\sum_{N=1}^{\infty} \Theta x_{MN}\, e^{i\omega t}\cos(\alpha x)\sin(\zeta y)\\
\phi_y(x,y,t) &= \sum_{M=1}^{\infty}\sum_{N=1}^{\infty} \Theta y_{MN}\, e^{i\omega t}\sin(\alpha x)\cos(\zeta y)
\end{aligned} \quad (20)$$

Where $\alpha = \frac{M\pi}{a}$ and $\zeta = \frac{N\pi}{b}$. $i = \sqrt{-1}$

Where U_{MN}, and V_{MN}, W_{MN}, $\Theta x_{MN,}$ Θy_{MN} are the arbitrary parameters and ω is the frequency of free vibration.

The transverse load (q) is also expanded as

$$q(x,y) = \sum_{M=1}^{\infty}\sum_{N=1}^{\infty} Q_{MN}\sin(\alpha x)\sin(\zeta y) \quad (21)$$

For loads acting on the (CNTRC) plates can be defined as

for sinusoidal load $Q_{MN} = q_0, (M = N = 1)$ (22)

for uniform load $Q_{MN} = \frac{16q_0}{MN\pi^2}, (M = N = 1,3,5....)$ (23)

Substituting the Eq. (20) into the Eq. (19), one obtains the closed-form solutions which are presented in the following matrix form.

$$\left([S] - \omega^2[M]\right)\begin{Bmatrix} U_{MN} \\ V_{MN} \\ W_{MN} \\ \Theta_{x\,MN} \\ \Theta_{y\,MN} \end{Bmatrix} = \begin{Bmatrix} 0 \\ 0 \\ q_{mn} \\ 0 \\ 0 \end{Bmatrix} \quad (24)$$

Where [M] and [S] are the global stiffness matrix and mass matrix respectively

$$\begin{aligned}
&m_{11} = m_{22} = m_{33} = -I_0,\ \ m_{44} = m_{55} = I_2,\ \ m_{12} = m_{21} = 0,\\
&m_{13} = m_{31} = 0,\ \ m_{14} = m_{41} = I_1,\ \ m_{15} = m_{51} = 0,\\
&m_{23} = m_{32} = 0,\ \ m_{24} = m_{42} = 0,\ \ m_{25} = m_{52} = I_1,\\
&m_{34} = m_{43} = 0,\ \ m_{35} = m_{53} = 0,\ \ m_{45} = m_{54} = 0,
\end{aligned} \quad (25)$$

And

$$\begin{aligned}
&s_{11} = -A_{11}\alpha^2 + A_{66}\zeta^2,\ \ s_{12} = -\alpha\zeta(A_{12} + A_{66}),\ \ s_{13} = 0,\\
&s_{14} = -B_{11}\alpha^3 - B_{66}\zeta^2,\ \ s_{15} = -B_{12}\alpha\zeta - B_{66}\alpha\zeta,\\
&s_{21} = s_{12},\ \ s_{22} = -A_{66}\alpha^2 - A_{22}\zeta^2,\ \ s_{23} = 0,\\
&s_{24} = -B_{12}\alpha\zeta - B_{66}\alpha\zeta,\ \ s_{25} = -B_{66}\alpha^2 - B_{22}\zeta^2,\\
&s_{31} = s_{13},\ \ s_{32} = s_{23},\ \ s_{33} = -D_{55}\alpha^2 - D_{44}\zeta^2,\\
&s_{34} = -D_{55}\alpha,\ \ s_{35} = -D_{44}\zeta,\ \ s_{41} = s_{14},\ \ s_{42} = s_{24},\\
&s_{43} = s_{34},\ \ s_{44} = -C_{11}\alpha^2 - C_{66}\zeta^2 - D_{55},\\
&s_{45} = -\alpha\zeta(C_{12} + C_{66}),\ \ s_{51} = s_{15},\ \ s_{52} = s_{25},\\
&s_{53} = s_{35},\ \ s_{54} = s_{45},\ \ s_{55} = -D_{44} - C_{66}\alpha^2 - C_{22}\zeta^2
\end{aligned} \quad (26)$$

For simplicity, the following non-dimensional parameters to present the numerical results for bending and vibration analyses of (CNTRC) plates are used:

For bending problem

$$\begin{aligned}
\overline{w} &= \frac{10^3 D_0}{q_0 a^4} w(a/2, b/2)\\
\overline{u} &= \frac{10^3 D_0}{q_0 a^4} u(0, b/2, -h/2)\\
\overline{v} &= \frac{10^3 D_0}{q_0 a^4} v(a/2, 0, -h/2)\\
\overline{\sigma}_{xx} &= -\frac{h^2}{q_0 a^2}\sigma_{xx}(a/2, b/2, -h/2)\\
\overline{\sigma}_{xy} &= \frac{h^2}{q_0 a^2}\sigma_{xy}(0, 0, -h/2)\\
\overline{\sigma}_{xz} &= -\frac{h^2}{q_0 a^2}\sigma_{xz}(0, b/2, -h/2)
\end{aligned} \quad (27)$$

Where $D_0 = \frac{E_0^P h^3}{12\left[1-(\nu^P)^2\right]}$

For vibration analysis

$$\overline{\omega} = \omega h\sqrt{\rho^P / E^P} \quad (28)$$

4. Numerical results and discussion

Numerical results for displacements, stresses, bending and free vibrations behaviors of (CNTRC) sandwich porous plates are presented in this section. The (CNTRC) sandwich porous plates are made of following material properties:

PMPV (Polymer) is used as the matrix in which material

properties are: $v^p = 0.34$, $\rho_0^p = 1150\, kg/m^3$ and $E_0^p = 2.1$ GPa. For reinforcement material, the armchair (10,10) SWCNTs is chosen with the following properties according to the study of Zhu et al. (2012):

$v_{12}^{cnt} = 0.175$; $\rho^{cnt} = 1400$ kg/m^3 ; $E_{11}^{cnt} = 5.6466\, TPa$; $E_{22}^{cnt} = 7.0800\, TPa$; $G_{12}^{cnt} = G_{13}^{cnt} = G_{23}^{cnt} = 1.9445\, TPa$.

To prove the validity of mathematical models in previous sections, a comparison is made between the present results and those from the open literature which were presented by Zhu *et al*. (2012) in Table 1. With different values of carbon nanotube volume fraction and various reinforcement of core or face sheet sandwich plate with porosity under uniform load are considered in this table with a thickness ratio of the plate (a/h = 10). It can be noted from this comparison the good agreement between the results without porosity. The face sheet (FG-CNTRC) reinforcement has a high resistance against deflections compared to other types of reinforcement. In addition, the

Table 1 Comparisons of dimensionless deflections $w^* = -(w_0/h)10^{-2}$ of square reinforced sandwich porous plate under uniform load

Reinforcement type		Core UD-CNT				Core FG-CNT			
V_{cnt}^*		Zhu *et al*. (2012)	Present			Zhu *et al*. (2012)	Present		
		P = 0	P = 0	P = 1%	P = 2%	P = 0	P = 0	P = 1%	P = 2%
0.11		0.3739	0.3739	0.4441	0.5812	0.5216	0.5228	0.6014	0.7470
0.14		0.3305	0.3298	0.3960	0.5264	0.4512	0.4512	0.5224	0.6573
0.17		0.2394	0.2394	0.2836	0.3699	0.3368	0.3377	0.3864	0.4768
		Face sheet UD-CNT				Face sheet FG-CNT			
0.11		0.3739	0.3739	0.4441	0.5812	0.3176	0.3177	0.3858	0.5206
0.14		0.3305	0.3298	0.3960	0.5264	0.2842	0.2838	0.3485	0.4768
0.17		0.2394	0.2394	0.2836	0.3699	0.2011	0.2013	0.2439	0.3282

Table 2 Convergence studies for deflections and stresses of square reinforced (1-2-1) sandwich plate with porosity under uniform load (V_{cnt}^* = 0.17, a/h = 10)

		Core reinforced sandwich plate						Top and bottom face sheet reinforced sandwich plate					
		UD-CNT			FG-CNT			UD-CNT			FG-CNT		
	M = N	P = 0	P = 1%	P = 2%	P = 0	P = 1%	P = 2%	P = 0	P = 1%	P = 2%	P = 0	P = 1%	P = 2%
$\bar{U}$	1	0.1971	0.2190	0.2465	0.2826	0.3296	0.3955	0.0427	0.0436	0.0447	0.0355	0.0362	0.0369
	5	0.1959	0.2166	0.2420	0.2836	0.3295	0.3929	0.0408	0.0415	0.0421	0.0339	0.0344	0.0348
	15	0.1959	0.2167	0.2420	0.2837	0.3295	0.3929	0.4086	0.0415	0.0421	0.0339	0.0344	0.0348
	35	0.1959	0.2167	0.2420	0.2837	0.3295	0.3929	0.4086	0.0415	0.0421	0.0339	0.0344	0.0348
	50	0.1959	0.2167	0.2420	0.2837	0.3295	0.3929	0.4086	0.0415	0.0421	0.0339	0.0344	0.0348
$\bar{W}$	1	1.5045	1.7420	2.1178	2.0192	2.4077	3.0141	0.5721	0.6829	0.8990	0.5257	0.6338	0.8462
	5	1.4480	1.6690	2.0129	1.9571	2.3281	2.9006	0.5257	0.6223	0.8105	0.4812	0.5757	0.7611
	15	1.4477	1.6687	0.2420	1.9568	2.3277	2.9001	0.5254	0.6219	0.8099	0.4809	0.5753	0.7605
	35	1.4477	1.6687	0.2420	1.9568	2.3277	2.9000	0.5254	0.6219	0.8099	0.4809	0.5753	0.7605
	50	1.4477	1.6687	0.2420	1.9568	2.3277	2.9000	0.5254	0.6219	0.8099	0.4809	0.5753	0.7605
$\bar{\sigma}_{xx}$	1	4.5810	5.0634	5.6666	-12.6524	-14.8119	-17.838	0.9993	1.0164	1.0344	1.6414	1.6691	1.6979
	5	4.2926	4.7413	5.2895	-11.8320	-13.8833	-16.733	0.9097	0.9202	0.9296	1.4944	1.5113	1.5270
	15	4.2899	4.7385	5.2866	-11.8232	-13.8739	-16.723	0.9091	0.9196	0.9290	1.4932	1.5104	1.5260
	35	4.2898	4.7384	5.2866	-11.8228	-13.8735	-16.722	0.9091	0.9196	0.9289	1.4932	1.5103	1.5260
	50	4.2898	4.7384	5.2866	-11.8228	-13.8735	-16.722	0.9091	0.9196	0.9289	1.4932	1.5103	1.5260
$\bar{\sigma}_{xy}$	1	0.8720	0.0743	0.0582	0.7481	0.0662	0.0541	0.0265	0.0226	0.0186	0.0297	0.0256	0.0213
	5	0.1017	0.0880	0.0710	0.8506	0.0759	0.0632	0.0366	0.0322	0.0276	0.0415	0.0369	0.0320
	15	0.1026	0.0889	0.0719	0.8566	0.0765	0.0637	0.0374	0.0330	0.0284	0.0425	0.0378	0.0329
	35	0.1027	0.0890	0.0719	0.8572	0.0765	0.0638	0.0375	0.0331	0.0284	0.0426	0.0379	0.0330
	50	0.1027	0.0890	0.0719	0.8573	0.0765	0.0638	0.0375	0.0331	0.0284	0.0426	0.0379	0.0330

results show that the deflection results increase as the percentage of porosity increase.

The different number of terms (M, N) are considered in Table 2 to give an idea of the convergence deflections, normal stresses and shear stresses results of square reinforced (1-2-1) sandwich plate with porosities under uniform load. It is concluded that the non-dimensional deflections for core and face sheets reinforced sandwich plate converge at 15th iteration for each of the (P = 0,1% and 2%), and stresses of the reinforced sandwich plate with porosities have been converged at 35th and 50th iterations for all porosities values. The dimensionless deflections ($\bar{W}$) of square reinforced 1-2-1 sandwich plate with porosities is obtained for various core or face sheet reinforcement, thickness ratio (a/h) and porosities coefficient under uniform loads are presented in table 3. As expected, it is observed that the dimensionless deflections decrease if the thickness ratio (a/h) increases for al reinforcement type. On the other hand, it can be seen that the (FG-CNTRC) face sheet reinforced sandwich plate with porosity has a high resistance against deflections because a concentration of the CNT at the top and bottom of sandwich porous plate.

Table 3 The effect of volume fraction of CNTs on the dimensionless deflections ($\bar{W}$) square reinforced 1-2-1 sandwich plate with porosity under uniform loads V_{cnt}^{*} = 0.11

Core reinforced sandwich plate						
	UD-CNT			FG-CNT		
a/*h*	P = 0	P = 1%	P = 2%	P = 0	P = 1%	P = 2r%
10	2.1638	2.5091	3.0480	2.8752	3.4437	4.3317
20	1.9383	2.1897	2.5288	2.6783	3.1671	3.8810
50	1.8744	2.0988	2.3806	2.6228	3.0890	3.7533
Top and bottom face sheet reinforced sandwich plate						
10	0.8067	0.9554	1.2446	0.7417	0.8875	1.1734
20	0.5024	0.5419	0.6130	0.4349	0.4719	0.5407
50	0.4152	0.4239	0.4342	0.3471	0.3535	0.3622

Table 4 Dimensionless deflections of square reinforced 1-2-1 sandwich plate with porosity under uniform and sinusoidal loads (V_{cnt}^{*} = 0.17)

			Core reinforced sandwich plate						Top and bottom face sheet reinforced sandwich plate					
			Uniform load			Sinusoidal load			Uniform load			Sinusoidal load		
	a/h	Schemes	P = 0	P = 1%	P = 2%	P = 0	P = 1%	P = 2%	P = 0	P = 1%	P = 2%	P = 0	P = 1%	P = 2%
$\bar{U}$	10	UD-CNT	0.1959	0.2167	0.2420	0.1189	0.1298	0.1429	0.0408	0.0415	0.0421	0.0229	0.0229	0.0229
		FG-CNT	0.2837	0.3295	0.3929	0.1749	0.2015	0.2375	0.0339	0.0344	0.0348	0.0189	0.0189	0.0189
	20	UD-CNT	0.1000	0.1108	0.1240	0.0620	0.0660	0.0725	0.0207	0.0209	0.0211	0.0111	0.0109	0.0105
		FG-CNT	0.1439	0.1676	0.2005	0.0884	0.1021	0.1206	0.0172	0.0173	0.0173	0.0091	0.0089	0.0085
	50	UD-CNT	0.0402	0.0446	0.0499	0.0242	0.0265	0.0291	0.0083	0.0083	0.0083	0.0043	0.0042	0.0039
		FG-CNT	0.0578	0.0673	0.0806	0.0355	0.0410	0.0484	0.0068	0.0069	0.0068	0.0035	0.0034	0.0031
$\bar{V}$	10	UD-CNT	0.2414	0.2828	0.3507	0.1695	0.2022	0.2583	0.1019	0.1238	0.1665	0.0830	0.1028	0.1418
		FG-CNT	0.3178	0.3818	0.4844	0.2159	0.2626	0.3405	0.0940	0.1151	0.1567	0.0769	0.0959	0.1335
	20	UD-CNT	0.1134	0.1298	0.1542	0.0813	0.0954	0.1186	0.0359	0.0408	0.0498	0.0332	0.0395	0.0512
		FG-CNT	0.1547	0.1836	0.2276	0.1060	0.1279	0.1632	0.0318	0.0363	0.0448	0.0299	0.0358	0.0467
	50	UD-CNT	0.0445	0.0505	0.0592	0.0321	0.0375	0.0463	0.0125	0.0137	0.0156	0.0124	0.0144	0.0180
		FG-CNT	0.0614	0.0673	0.0893	0.0422	0.0507	0.0645	0.0108	0.0118	0.0136	0.0110	0.0128	0.0161
$\bar{W}$	10	UD-CNT	1.4477	1.6687	2.0123	0.8373	0.9573	1.1374	0.5254	0.6219	0.8099	0.2782	0.3239	0.4126
		FG-CNT	1.9568	2.3277	2.9000	1.1462	1.3577	1.6770	0.4809	0.5753	0.7605	0.2529	0.2978	0.3858
	20	UD-CNT	1.3029	1.4628	1.6763	0.7586	0.8443	0.9511	0.3277	0.3531	0.3991	0.1688	0.1760	0.1891
		FG-CNT	1.8319	2.1518	2.6118	1.0799	1.2633	1.5202	0.2830	0.3069	0.3514	0.1436	0.1505	0.1638
	50	UD-CNT	1.2619	1.4043	1.5803	0.7362	0.8120	0.8977	0.2711	0.2763	0.2826	0.1379	0.1348	0.1287
		FG-CNT	1.7968	2.1022	2.5302	1.0612	1.2366	1.4755	0.2263	0.2303	0.2357	0.1128	0.1098	0.1046

Table 5 Comparisons of dimensionless frequencies ($\bar{\omega}$) of square reinforced sandwich plate with porosity under uniform loads (V_{cnt}^{*} = 0.17, a/h = 10)

Core reinforced sandwich plate								
Reinforcement type	UD-CNT				FG-CNT			
	Wattanasakulpong and Chaikittiratana (2015)TSDT	Present			Wattanasakulpong and Chaikittiratana (2015)TSDT	Present		
(m,n)	P = 0	P = 0	P = 1%	P = 2%	P = 0	P = 0	P = 1%	P = 2%
(1-1)	0.1683	0.1678	0.1716	0.1726	0.1409	0.1425	0.1483	0.1533
(1-2)	0.2201	0.2196	0.2187	0.2137	0.1993	0.1999	0.2001	0.1976
(2-2)	0.4383	0.4305	0.4241	0.4074	0.3992	0.4048	0.4035	0.3932
Top and bottom face sheet reinforced sandwich plate								
(1-1)	0.1683	0.1678	0.1716	0.1726	0.1819	0.1824	0.1845	0.1829
(1-2)	0.2201	0.2196	0.2187	0.2137	0.2334	0.2343	0.2321	0.2249
(2-2)	0.4383	0.4305	0.4241	0.4074	0.4524	0.4463	0.4374	0.4176

Table 6 Effect of aspect ratio a/h on the dimensionless deflection and stresses of square reinforced sandwich plate with porosity for various schemes under uniform load (V_{cnt}^{*} = 0.17)

			Core reinforced sandwich plate						Top and bottom face sheet reinforced sandwich plate					
	a/h	Schemes	UD-CNT			FG-CNT			UD-CNT			FG-CNT		
			P = 0	P = 1%	P = 2%	P = 0	P = 1%	P = 2%	P = 0	P = 1%	P = 2%	P = 0	P = 1	P = 2%
$\bar{U}$	10	1-1-1	0.3452	0.4158	0.5228	0.4123	0.5164	0.6913	0.0374	0.0379	0.0384	0.0289	0.0291	0.0294
		1-2-1	0.1959	0.2167	0.2420	0.2837	0.3295	0.3929	0.0409	0.0415	0.0421	0.0339	0.0344	0.0348
		2-1-2	0.4636	0.5988	0.8461	0.4875	0.6390	0.9274	0.0364	0.0369	0.0373	0.0265	0.0267	0.0270
	20	1-1-1	0.1743	0.2105	0.2657	0.2071	0.2599	0.3490	0.0190	0.0191	0.0191	0.0146	0.0146	0.0146
		1-2-1	0.1000	0.1108	0.1240	0.1439	0.1676	0.2005	0.0208	0.0209	0.0211	0.0172	0.0173	0.0173
		2-1-2	0.2319	0.2999	0.4247	0.2435	0.3193	0.4640	0.0184	0.0185	0.0186	0.0134	0.0134	0.0134
$\bar{W}$	10	1-1-1	2.3135	2.8333	3.6720	2.6833	3.3962	4.6314	0.4962	0.5890	0.7705	0.4413	0.5318	0.7100
		1-2-1	1.4477	1.6687	2.0123	1.9568	2.3277	2.9000	0.5254	0.6219	0.8099	0.4809	0.5753	0.7605
		2-1-2	2.9582	3.8449	5.4923	3.0783	4.0498	5.9174	0.4839	0.5744	0.7513	0.4204	0.5082	0.6816
	20	1-1-1	2.1931	2.6669	3.4043	2.5690	3.2416	4.3917	0.3030	0.3268	0.3706	0.2480	0.2703	0.3126
		1-2-1	1.3029	1.4628	1.6763	1.8320	2.1518	2.6118	0.3277	0.3531	0.3991	0.2830	0.3069	0.3514
		2-1-2	2.8417	3.6893	5.2574	2.9621	3.8950	5.6852	0.2948	0.3178	0.3603	0.2312	0.2525	0.2935
$\bar{\sigma}_{xx}$	10	1-1-1	7.3480	8.8764	11.213	-33.3294	-42.2228	-57.370	0.8317	0.8397	0.8467	1.2707	1.2822	1.2924
		1-2-1	4.2898	4.7384	5.2865	-11.8228	-13.8735	-16.722	0.9091	0.9196	0.9289	1.4932	1.5103	1.5260
		2-1-2	9.4161	12.193	17.348	-75.9566	-100.241	-147.06	0.8092	0.8165	0.8227	1.1675	1.1767	1.1848
	20	1-1-1	7.4237	8.9938	11.411	-33.4862	-42.5136	-57.973	0.8402	0.8429	0.8412	1.2823	1.5200	1.5197
		1-2-1	4.3829	4.8519	5.4229	-12.0062	-14.1301	-17.096	0.9209	0.9260	0.9262	1.5126	1.2848	1.2812
		2-1-2	9.4215	12.214	17.415	-75.8651	-100.181	-147.14	0.8165	0.8185	0.8162	1.1757	1.1764	1.1718
$\bar{\sigma}_{xy}$	10	1-1-1	0.1632	0.1498	0.1294	0.0940	0.0890	0.0807	0.0357	0.0315	0.0272	0.0391	0.0350	0.0307
		1-2-1	0.1027	0.0891	0.0720	0.0857	0.0765	0.0638	0.0375	0.0331	0.0285	0.0426	0.0379	0.0330
		2-1-2	0.2106	0.2048	0.1944	0.0775	0.0763	0.0741	0.0350	0.0309	0.0267	0.0372	0.0334	0.0295
	20	1-1-1	0.1619	0.0848	0.0668	0.0937	0.0749	0.0616	0.0282	0.0237	0.0188	0.0296	0.0279	0.0223
		1-2-1	0.0992	0.1481	0.1270	0.0845	0.0886	0.0801	0.0301	0.0252	0.0200	0.0331	0.0250	0.0201
		2-1-2	0.2105	0.2046	0.1940	0.0775	0.0763	0.0740	0.0277	0.0232	0.0185	0.0278	0.0236	0.0190

Table 4 presents a comparison of dimensionless deflections ($\bar{W}$) of square reinforced 1-2-1 sandwich porous plate for various parameters such as carbon nanotube volume fraction, uniform and sinusoidal loads, various reinforcement of core or face sheet porous plate and porosity percentage. It can be concluded from the results of the table that the deflections of plates under uniform load have large values compared to plates subjected to sinusoidal load. As we conclude that the increase in the porosity coefficient leads to increase of the dimensionless deflections.

To validate the results of dimensionless frequencies mathematical models, a comparison between the results obtained and the existing ones in the literature which were presented by Zhu *et al*. (2012) are presented in Table 5. The effect of the various number of mode on the dimensionless frequency ($\bar{\omega}$) of square reinforced sandwich porous plate are also presented in this table under uniform loads with (V_{cnt}^{*} = 0.17). The small variation in frequency between the Wattanasakulpong and Chaikittiratana (2015) and present results is due to the higher-order shear deformation model proposed by Wattanasakulpong and Chaikittiratana (2015). However, it is deduced that the dimensionless frequencies increase by increasing the number of modes. Also, the results reveal that the dimensionless frequency results increase as the porosity increases.

Table 6 presents the effect of various schemes or thickness of layer sandwich plate under porosity and various aspect ratio a/h on the dimensionless deflection and stresses of square reinforced sandwich porous plate with (V_{cnt}^{*} = 0.17). It can be seen that the ranges of dimensionless deflection and stresses for various schemes or thickness of layer sandwich plate with porosity are quite different, in the case of core reinforced sandwich porous plate the range is the smallest for (1-2-1) schemes, but the range is the largest for (2-1-2) and the opposite in the case

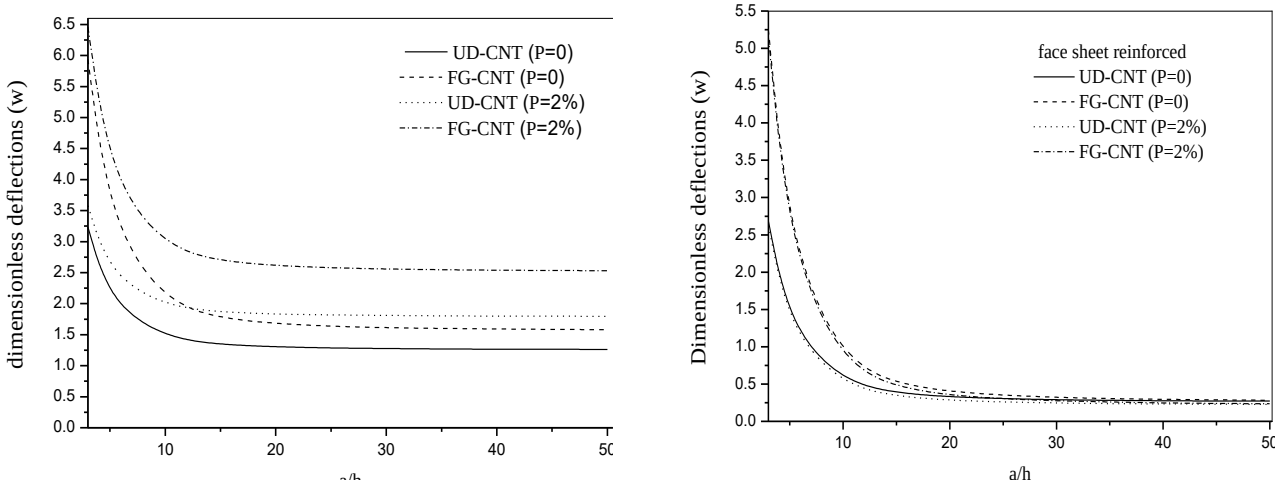

(a) Core 1-2-1 reinforced sandwich plate. (b) Face sheet 1-2-1 reinforced sandwich plate

Fig. 3 Effect of aspect ratio a/h on the dimensionless deflection ($\bar{W}$) of square face sheet reinforced 1-2-1 sandwich plate under uniform load (V_{cnt}^{*} = 0.17) and porosity coefficient (P)

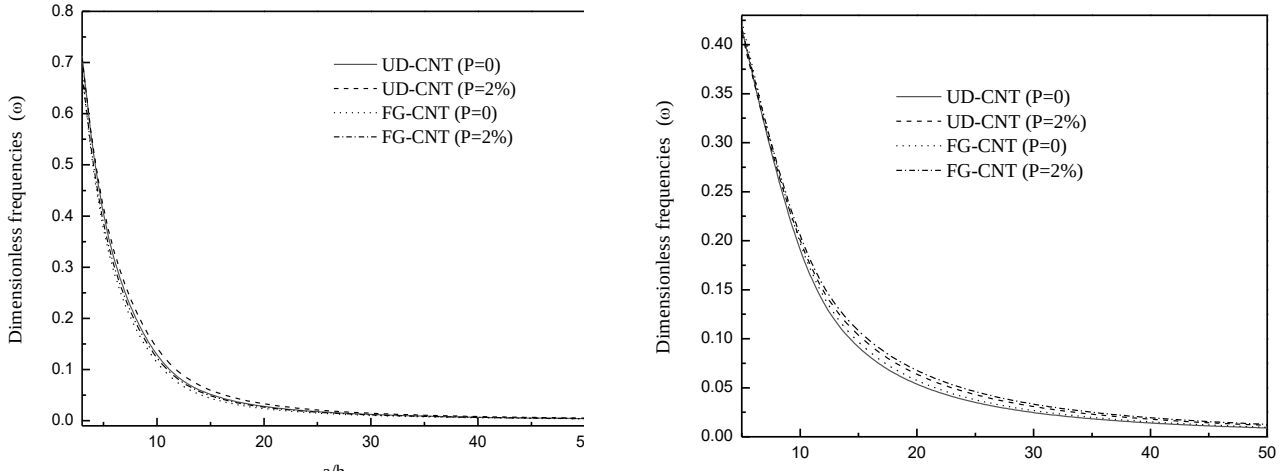

(a) Core 1-2-1 reinforced sandwich plate (b) Face sheet1-2-1 reinforced sandwich plate

Fig. 5 Dimensionless first frequencies of square reinforced sandwich plate under uniform load (V_{cnt}^{*} = 0.17)

of top and bottom face sheet reinforced sandwich porous plate. The reason for this difference is attributed to the increasing or decreasing of the thickness of reinforced layers.

The dimensionless deflection ($\bar{W}$) of square reinforced 1-2-1 sandwich plate with porosity under uniform load with four various reinforced types is illustrated in the (Fig. 3) to analyze the effect of aspect ratio a/h and porosity coefficient. Observing the figure, it is easily deduced that as the aspect ratio increase, the dimensionless deflection decrease then it stabilizes for the higher value of aspect ratio (a/h > 20). The reason for this stability is attributed to the effect of shear stress.

It can be concluded that the large difference between the face sheet and core reinforced sandwich plate with porosity is attributed to a concentration of (CNT) at the top and bottom face sheet layer, Furthermore, an increase of the porosity coefficient leads to increase of the dimensionless deflection.

The variation of dimensionless first frequencies of square reinforced core and face sheet 1-2-1 sandwich plate with porosity under uniform load with volume fraction (V_{cnt}^{*} = 0.17) of CNT are presented in (Fig. 4) respectively. Their results show the dependence of dimensionless frequencies with aspect Ratio, porosity coefficient and various reinforcement type of sandwich porous plate. In this case, It can be seen that the difference between the dimensionless frequency of (UD-CNTRC) and (FG-CNTRC) it is very weak. Also, the range of the dimensionless frequency decrease with increasing aspect ratio (a/h). On the other hand, the reduction in the dimensionless frequency is most pronounced in core reinforced sandwich plate with porosity for the values of aspect ratio (a/h > 5).

5. Conclusions

In this work, the influence of different parameters on the static and dynamic behavior of carbon nanotube-reinforced composite sandwich plates with porosity using the first-order shear deformation theory (FSDT) are studied and discussed.

The governing differential equations include the different parameters are solved by implementing Hamilton's principle and the dimensionless bending, stresses and vibration analyses of two types of sandwich plates with porosity are obtained. Accuracy of the results is examined using an available date in the literature. Finally, through some parametric investigated study the results showed the dependence of static and dynamic behavior on the different parameters such as aspect ratios, volume fraction, types of reinforcement and plate thickness for two values of porosity. From the numerical results, it is concluded that the concentration of the nanotubes at the top and bottom of the (FG-CNTRC) face sheet reinforced sandwich plate conduce to high resistance against deflections compared to other types of reinforcement In terms of deflection and vibration analyses, the results show:

- With the increase the percentage of porosity the deflection increases for every porous plate type.
- It can be seen that the deflections of plates under uniform load have large values compared to plates subjected to sinusoidal load.
- As we conclude that the dimensionless frequencies increase by increasing the number of mode and porosity.
- The results reveal that the ranges of dimensionless deflection and stresses for various schemes or thickness of layer sandwich plate with porosity are quite different, in the case of core reinforced sandwich porous plate the range is the smallest for (1-2-1) schemes, but the range is the largest for (2-1-2) and the opposite in the case of top and bottom face sheets reinforced sandwich porous plate. The reason for this difference is attributed to the increasing or decreasing of the thickness of reinforced layers.
- As the aspect ratio increase, the dimensionless deflection decrease then it stabilizes for the higher value of aspect ratio (a/h > 20). The reason for this stability is attributed to the effect of shear stress

Finally, the results demonstrate the dependence of static and dynamic behavior on the different parameters such as aspect ratios, volume fraction, porosity, types of reinforcement and plate thickness.

References

Abdelaziz, H.H., Meziane, M.A.A, Bousahla, A.A., Tounsi, A., Mahmoud, S.R. and Alwabli, A.S. (2017), "An efficient hyperbolic shear deformation theory for bending, buckling and free vibration of FGM sandwich plates with various boundary conditions", *Steel Compos. Struct., Int. J.*, **25**(6), 693-704. https://doi.org/10.12989/scs.2017.25.6.693

Abualnour, M., Houari, M.S.A., Tounsi, A., AddaBedia, E.A., Mahmoud, S.R. (2018), "A novel quasi 3D trigonometric plate theory for free vibration analysis of advanced composite plates", *Compos. Struct.*, **184**, 688-697. https://doi.org/10.1016/j.compstruct.2017.10.047

Ahouel, M., Houari, M.S.A., Adda Bedia, E.A. and Tounsi, A. (2016), "Size-dependent mechanical behavior of functionally graded trigonometric shear deformable nanobeams including neutral surface position concept", *Steel Compos. Struct., Int. J.*, **20**(5), 963-981. https://doi.org/10.12989/scs.2016.20.5.963

Ait Atmane, H, Tounsi, A. and Bernard, F. (2017), "Effect of thickness stretching and porosity on mechanical response of a functionally graded beams resting on elastic foundations", *Int. J. Mech. Mater. Des.*, **13**(1), 71-84. https://doi.org/10.1007/s10999-015-9318-x

Ait Yahia, S., Ait Atmane, H., Houari, M.S.A. and Tounsi, A. (2015), "Wave propagation in functionally graded plates with porosities using various higher-order shear deformation plate theories", *Struct. Eng. Mech., Int. J.*, **53**(6), 1143-1165. https://doi.org/10.12989/sem.2015.53.6.1143

Ajayan, P.M., Stephen, O., Colliex, C. and Trauth, D. (1994), "Aligned carbon nanotube arrays formed by cutting a polymer resin-nanotube composite", *Science*, **256**, 1212-1214. https://doi.org/10.1126/science.265.5176.1212

Akgoz, B. and Civalek, O. (2011), "Nonlinear vibration analysis of laminated plates resting on nonlinear two-parameters elastic

foundations", *Steel Compos. Struct., Int. J.*, **11**(5), 403-421. https://doi.org/10.12989/scs.2011.11.5.403

Alankaya, V. and Erdonmez, C. (2017), "Bending performance of laminated sandwich shells in hyperbolic paraboloidal form", *Steel Compos. Struct., Int. J.*, **25**(3), 337-346. https://doi.org/10.12989/scs.2017.25.3.337

Allahkarami, F., Nikkhah-Bahrami, M. and Saryazdi, M.G. (2017), "Damping and vibration analysis of viscoelastic curved microbeam reinforced with FG-CNTs resting on viscoelastic medium using strain gradient theory and DQM", *Steel Compos. Struct., Int. J.*, **25**(2), 141-155. https://doi.org/10.12989/scs.2017.25.2.141

Asadi, H. and Wang, Q. (2017), "Dynamic stability analysis of a pressurized FG-CNTRC cylindrical shell interacting with supersonic airflow", *Compos. Part B: Eng.*, **118**, 15-25. https://doi.org/10.1016/j.compositesb.2017.03.001

Attia, A., Bousahla, A.A., Tounsi, A., Mahmoud, S.R. and Alwabli, A.S. (2018), "A refined four variable plate theory for thermoelastic analysis of FGM plates resting on variable elastic foundations", *Struct. Eng. Mech., Int. J.*, **65**(4), 453-464. https://doi.org/10.12989/sem.2018.65.4.453

Avcar, M. (2015), "Effects of rotary inertia shear deformation and non-homogeneity on frequencies of beam", *Struct. Eng. Mech., Int. J.*, **55**(4), 871-884. https://doi.org/10.12989/sem.2015.55.4.871

Avcar, M. (2016), "Effects of material non-homogeneity and two parameter elastic foundation on fundamental frequency parameters of Timoshenko beams", *Acta Physica Polonica A*, **130**(1), 375-378. https://doi.org/10.12693/APhysPolA.130.375

Avcar, M. (2019), "Free vibration of imperfect sigmoid and power law functionally graded beams", *Steel Compos. Struct., Int. J.*, **30**(6), 603-615. https://doi.org/10.12989/scs.2019.30.6.603

Avcar, M. and Alwan, H.H.A. (2017), "Free vibration of functionally graded Rayleigh beam", *Int. J. Eng. Appl. Sci.*, **9**(2), 127-137. http://dx.doi.org/10.24107/ijeas.322884

Avcar, M. and Mohammed, W.K.M. (2018), "Free vibration of functionally graded beams resting on Winkler-Pasternak foundation", *Arab. J. Geosci.*, **11**(10), 232. https://doi.org/10.1007/s12517-018-3579-2

Bakhadda, B., Bouiadjra, M.B., Bourada, F., Bousahla, A.A., Tounsi, A. and Mahmoud, S.R. (2018), "Dynamic and bending analysis of carbon nanotube-reinforced composite plates with elastic foundation", *Wind Struct., Int. J.*, **27**(5), 311-324. https://doi.org/10.12989/was.2018.27.5.311

Baltacioglu, A.K. and Civalek, O. (2018), "Numerical approaches for vibration response of annular and circular composite plates", *Steel Compos. Struct., Int. J.*, **29**(6), 755-766. https://doi.org/10.12989/scs.2018.29.6.759

Baseri, V., Jafari, G.S. and Kolahchi, R. (2016), "Analytical solution for buckling of embedded laminated plates based on higher order shear deformation plate theory", *Steel Compos. Struct., Int. J.*, **21**(4), 883-919. https://doi.org/10.12989/scs.2016.21.4.883

Belabed, Z., Bousahla, A.A., Houari, M.S.A., Tounsi, A. and Mahmoud, S.R. (2018), "A new 3-unknown hyperbolic shear deformation theory for vibration of functionally graded sandwich plate", *Earthq. Struct., Int. J.*, **14**(2), 103-115. https://doi.org/10.12989/eas.2018.14.2.103

Beldjelili, Y., Tounsi, A. and Mahmoud, S.R. (2016), "Hygro-thermo mechanical bending of S-FGM plates resting on variable elastic foundations using a four-variable trigonometric plate theory", *Smart Struct. Syst., Int. J.*, **18**(4), 755-786. https://doi.org/10.12989/sss.2016.18.4.755

Belkacem, A., Tahar, H.D., Abderrezak, R., Amine, B.M., Mohamed, Z. and Boussad, A. (2018), "Mechanical buckling analysis of hybrid laminated composite plates under different boundary conditions", *Struct. Eng. Mech., Int. J.*, **66**(6), 761-769. https://doi.org/10.12989/sem.2018.66.6.761

Bellifa, H., Bakora, A., Tounsi, A., Bousahla, A.A. and Mahmoud, S.R. (2017a), "An efficient and simple four variable refined plate theory for buckling analysis of functionally graded plates", *Steel Compos. Struct., Int. J.*, **25**(3), 257-270. https://doi.org/10.12989/scs.2017.25.3.257

Bellifa, H., Benrahou, K.H., Bousahla, A.A., Tounsi, A. and Mahmoud, S.R. (2017b), "A nonlocal zeroth-order shear deformation theory for nonlinear postbuckling of nanobeams", *Struct. Eng. Mech., Int. J.*, **62**(6), 695-702. https://doi.org/10.12989/sem.2017.62.6.695

Belmahi, S., Zidour, M., Meradjah, M., Bensattalah, T. and Dihaj, A. (2018), "Analysis of boundary conditions effects on vibration of nanobeam in a polymeric matrix", *Struct. Eng. Mech., Int. J.*, **67**(5), 517-525. https://doi.org/10.12989/sem.2018.67.5.517

Belmahi, S., Zidour, M. and Meradjah, M. (2019), "Small-scale effect on the forced vibration of a nano beam embedded an elastic medium using nonlocal elasticity theory", *Adv. Aircr. Spacecr. Sci.*, **6**(1), 1-18. https://doi.org/10.12989/aas.2019.6.1.001

Benahmed, A., Fahsi, B., Benzair, A., Zidour, M., Bourada, F. and Tounsi, A. (2019), "Critical buckling of functionally graded nanoscale beam with porosities using nonlocal higher-order shear deformation", *Struct. Eng. Mech., Int. J.*, **69**(4), 457-466. https://doi.org/10.12989/sem.2019.69.4.457

Benchohra, M., Driz, H., Bakora, A., Tounsi, A., Adda Bedia, E.A. and Mahmoud, S.R. (2018), "A new quasi-3D sinusoidal shear deformation theory for functionally graded plates", *Struct. Eng. Mech., Int. J.*, **65**(1), 19-31. https://doi.org/10.12989/sem.2018.65.1.019

Bensattalah, T., Daouadji, T.H., Zidour, M., Tounsi, A. and Bedia, E.A. (2016), "Investigation of thermal and chirality effects on vibration of single-walled carbon nanotubes embedded in a polymeric matrix using nonlocal elasticity theories", *Mech. Compos. Mater.*, **52**(4), 555-568. https://doi.org/10.1007/s11029-016-9606-z

Bensattalah, T., Bouakkaz, K., Zidour, M. and Daouadji, T.H. (2018a), "Critical buckling loads of carbon nanotube embedded in Kerr's medium", *Adv. Nano Res., Int. J.*, **6**(4), 339-356. https://doi.org/10.12989/anr.2018.6.4.339

Bensattalah, T., Zidour, M. and Hassaine Daouadji, T. (2018b), "Analytical analysis for the forced vibration of CNT surrounding elastic medium including thermal effect using nonlocal Euler-Bernoulli theory", *Adv. Mater. Res., Int. J.*, **7**(3), 163-174. https://doi.org/10.12989/amr.2018.7.3.163

Bensattalah, T., Zidour, M., Hassaine Daouadji, T. and Bouakaz, K. (2019), "Theoretical analysis of chirality and scale effects on critical buckling load of zigzag triple walled carbon nanotubes under axial compression embedded in polymeric matrix", *Struct. Eng. Mech., Int. J.*, **70**(3), 269-277. https://doi.org/10.12989/sem.2019.70.3.269

Bouadi, A., Bousahla, A.A., Houari, M.S.A., Heireche, H. and Tounsi, A. (2018), "A new nonlocal HSDT for analysis of stability of single layer graphene sheet", *Adv. Nano Res., Int. J.*, **6**(2), 147-162. https://doi.org/10.12989/anr.2018.6.2.147

Bouazza, M., Amara, K., Zidour, M., Tounsi, A. and Adda-Bedia, E.A. (2015), "Postbuckling Analysis of Functionally Graded Beams Using Hyperbolic Shear Deformation Theory", *Rev. Info. Eng. Appl.*, **2**(1), 1-14. https://doi.org/10.18488/journal.79/2015.2.1/79.1.1.14

Bouhadra, A., Tounsi, A., Bousahla, A.A., Benyoucef, S. and Mahmoud, S.R. (2018), "Improved HSDT accounting for effect of thickness stretching in advanced composite plates", *Struct. Eng. Mech., Int. J.*, **66**(1), 61-73. https://doi.org/10.12989/sem.2018.66.1.061

Boukhlif, Z., Bouremana, M., Bourada, F., Bousahla, A.A.,

Bourada, M., Tounsi, A. and Al-Osta, M.A. (2019), "A simple quasi-3D HSDT for the dynamics analysis of FG thick plate on elastic foundation", *Steel Compos. Struct., Int. J.*, **31**(5), 503-516. https://doi.org/10.12989/scs.2019.31.5.503

Boulefrakh, L., Hebali, H., Chikh, A., Bousahla, A.A., Tounsi, A. and Mahmoud, S.R. (2019), "The effect of parameters of visco-Pasternak foundation on the bending and vibration properties of a thick FG plate", *Geomech. Eng., Int. J.*, **18**(2), 161-178. https://doi.org/10.12989/gae.2019.18.2.161

Bounouara, F., Benrahou, K.H., Belkorissat, I. and Tounsi, A. (2016), "A nonlocal zeroth-order shear deformation theory for free vibration of functionally graded nanoscale plates resting on elastic foundation", *Steel Compos. Struct., Int. J.*, **20**(2), 227-249. https://doi.org/10.12989/scs.2016.20.2.227

Bourada, F., Amara, K., Bousahla, A.A., Tounsi, A. and Mahmoud, S.R. (2018), "A novel refined plate theory for stability analysis of hybrid and symmetric S-FGM plates", *Struct. Eng. Mech., Int. J.*, **68**(6), 661-675. https://doi.org/10.12989/sem.2018.68.6.661

Bourada, F., Bousahla, A.A., Bourada, M., Azzaz, A., Zinata, A. and Tounsi, A. (2019), "Dynamic investigation of porous functionally graded beam using a sinusoidal shear deformation theory", *Wind Struct., Int. J.*, **28**(1), 19-30. https://doi.org/10.12989/was.2019.28.1.019

Bousahla, A.A., Benyoucef, S., Tounsi, A. and Mahmoud, S.R. (2016), "On thermal stability of plates with functionally graded coefficient of thermal expansion", *Struct. Eng. Mech., Int. J.*, **60**(2), 313-335. https://doi.org/10.12989/sem.2016.60.2.313

Boutaleb, S., Benrahou, K.H., Bakora, A., Algarni, A., Bousahla, A.A., Tounsi, A., Mahmoud, S.R. and Tounsi, A. (2019), "Dynamic Analysis of nanosize FG rectangular plates based on simple nonlocal quasi 3D HSDT", *Adv. Nano Res., Int. J.*, **7**(3), 189-206. https://doi.org/10.12989/anr.2019.7.3.189

Chaabane, L.A., Bourada, F., Sekkal, M., Zerouati, S., Zaoui, F.Z., Tounsi, A., Derras, A., Bousahla, A.A. and Tounsi, A. (2019), "Analytical study of bending and free vibration responses of functionally graded beams resting on elastic foundation", *Struct. Eng. Mech., Int. J.*, **71**(2), 185-196. https://doi.org/10.12989/sem.2019.71.2.185

Chemi, A., Heireche, H., Zidour, M., Rakrak, K. and Bousahla, A.A. (2015), "Critical buckling load of chiral double-walled carbon nanotube using non-local theory elasticity", *Adv. Nano Res., Int. J.*, **3**(4), 193-206. https://doi.org/10.12989/anr.2015.3.4.193

Chemi, A., Zidour, M., Heireche, H., Rakrak, K. and Bousahla, A.A. (2018), "Critical buckling load of chiral double-walled carbon nanotubes embedded in an elastic medium", *Mech. Compos. Mater.*, **53**(6), 827-836. https://doi.org/10.1007/s11029-018-9708-x

Chen, D., Yang, J. and Kitipornchai, S. (2017), "Nonlinear vibration and postbuckling of functionally graded graphene reinforced porous nanocomposite beams", *Compos. Sci. Technol.*, **142**, 235-245. https://doi.org/10.1016/j.compscitech.2017.02.008

Cherif, R.H., Meradjah, M., Zidour, M., Tounsi, A., Belmahi, H. and Bensattalah, T. (2018), "Vibration analysis of nano beam using differential transform method including thermal effect", *J. Nano Res.*, **54**, 1-14.

Chikh, A., Tounsi, A., Hebali, H. and Mahmoud, S.R. (2017), "Thermal buckling analysis of cross-ply laminated plates using a simplified HSDT", *Smart Struct. Syst., Int. J.*, **19**(3), 289-297. https://doi.org/10.12989/sss.2017.19.3.289

Costa, M.L., De Almeida, S.F.M. and Rezende, M.C. (2001), "The influence of porosity on the interlaminar shear strength of carbon/epoxy and carbon/bismaleimide fabric laminates", *Compos. Sci. Technol.*, **61**(14), 2101-2108. https://doi.org/10.1016/S0266-3538(01)00157-9

Dash, S., Mehar, K., Sharma, N., Mahapatra, T.R. and Panda, S.K. (2018), "Modal analysis of FG sandwich doubly curved shell structure", *Struct. Eng. Mech., Int. J.*, **68**(6), 721-733. https://doi.org/10.12989/sem.2018.68.6.721

Dash, S., Mehar, K., Sharma, N., Mahapatra, T.R. and Panda, S.K. (2019), "Finite element solution of stress and flexural strength of functionally graded doubly curved sandwich shell panel", *Earthq. Struct., Int. J.*, **16**(1), 55-67. https://doi.org/10.12989/eas.2019.16.1.055

Dihaj, A., Zidour, M., Meradjah, M., Rakrak, K., Heireche, H. and Chemi, A. (2018), "Free vibration analysis of chiral double-walled carbon nanotube embedded in an elastic medium using non-local elasticity theory and Euler Bernoulli beam model", *Struct. Eng. Mech., Int. J.*, **65**(3), 335-342. https://doi.org/10.12989/sem.2018.65.3.335

Draiche, K., Tounsi, A. and Mahmoud, S.R. (2016), "A refined theory with stretching effect for the flexure analysis of laminated composite plates", *Geomech. Eng., Int. J.*, **11**(5), 671-690. https://doi.org/10.12989/gae.2016.11.5.671

Draoui, A., Zidour, M., Tounsi, A. and Adim, B. (2019), "Static and dynamic behavior of nanotubes-reinforced sandwich plates using (FSDT)", *J. Nano Res.*, **57**, 117-135.

Dresselhaus, M.S. and Avouris, P. (2001), "Carbon nanotubes: synthesis, structure, properties and application", *Top Appl. Phys.*, **80**, 1-11. https://doi.org/10.1007/3-540-39947-X

El-Haina, F., Bakora, A., Bousahla, A.A., Tounsi, A. and Mahmoud, S.R. (2017), "A simple analytical approach for thermal buckling of thick functionally graded sandwich plates", *Struct. Eng. Mech., Int. J.*, **63**(5), 585-595. https://doi.org/10.12989/sem.2017.63.5.585

Fourn, H., AitAtmane, H., Bourada, M., Bousahla, A.A., Tounsi, A. and Mahmoud, S.R. (2018), "A novel four variable refined plate theory for wave propagation in functionally graded material plates", *Steel Compos. Struct., Int. J.*, **27**(1), 109-122. https://doi.org/10.12989/scs.2018.27.1.109

Ghiorse, S.R. (1993), "Effect of void content on the mechanical properties of carbon/epoxy laminates", *Samp. Quarter.*, **1**, 54-59.

Guessas, H., Zidour, M., Meradjah, M. and Tounsi, A. (2018), "The critical buckling load of reinforced nanocomposite porous plates", *Struct. Eng. Mech., Int. J.*, **67**(2), 115-123. https://doi.org/10.12989/sem.2018.67.2.115

Hajmohammad, M.H., Zarei, M.S., Farrokhian, A. and Kolahchi, R. (2018), "A layerwise theory for buckling analysis of truncated conical shells reinforced by CNTs and carbon fibers integrated with piezoelectric layers in hygrothermal environment", *Adv. Nano Res., Int. J.*, **6**(4), 299-321. https://doi.org/10.12989/anr.2018.6.4.299

Hamidi, A., Zidour, M., Bouakkaz, K. and Bensattalah, T. (2018), "Thermal and small-scale effects on vibration of embedded armchair single-walled carbon nanotubes", *J. Nano Res.*, **51**, 24-38. https://doi.org/10.4028/www.scientific.net/JNanoR.51.24

Hamza-Cherif, R., Meradjah, M., Zidour, M., Tounsi, A., Belmahi, S. and Bensattalah, T. (2018), "Vibration analysis of nano beam using differential transform method including thermal effect", *J. Nano Res.*, **54**, 1-14. https://doi.org/10.4028/www.scientific.net/JNanoR.54.1

Hu, J.S. and Hwu, C. (1995), "Free vibration of delaminated composite sandwich beams", *AIAA J.*, **33**(10), 1911-1918. https://doi.org/10.2514/3.12745

Iijima, S. (1991), "Helical microtubules of graphitic carbon", *Nature*, **354**, 56-58. https://doi.org/10.1038/354056a0

Kaci, A., Houari, M.S.A., Bousahla, A.A., Tounsi, A. and Mahmoud, S.R. (2018), "Post-buckling analysis of shear-deformable composite beams using a novel simple two-unknown beam theory", *Struct. Eng. Mech., Int. J.*, **65**(5), 621-631. https://doi.org/10.12989/sem.2018.65.5.621

Kadari, B., Bessaim, A., Tounsi, A., Heireche, H., Bousahla, A.A. and Houari, M.S.A. (2018), "Buckling analysis of orthotropic nanoscale plates resting on elastic foundations", *J. Nano Res.*, **55**, 42-56. https://doi.org/10.4028/www.scientific.net/JNanoR.55.42

Kar, V.R. and Panda, S.K. (2015), "Large deformation bending analysis of functionally graded spherical shell using FEM", *Struct. Eng. Mech., Int. J.*, **53**(4), 661-679. https://doi.org/10.12989/sem.2015.53.4.661

Karami, B., Janghorban, M. and Li, L. (2018a), "On guided wave propagation in fully clamped porous functionally graded nanoplates", *Acta Astronautica*, **143**, 380-390. https://doi.org/10.1007/s12206-015-0811-9

Karami, B., Janghorban, M., Shahsavari, D. and Tounsi, A. (2018b), "A size-dependent quasi-3D model for wave dispersion analysis of FG nanoplates", *Steel Compos. Struct., Int. J.*, **28**(1), 99-110. https://doi.org/10.12989/scs.2018.28.1.099

Katariya, P.V., Panda, S.K., Hirwani, C.K., Mehar, K. and Thakare, O. (2017), "Enhancement of thermal buckling strength of laminated sandwich composite panel structure embedded with shape memory alloy fibre", *Smart Struct. Syst., Int. J.*, **20**(5), 595-605. https://doi.org/10.12989/sss.2017.20.5.595

Khetir, H., BachirBouiadjra, M., Houari, M.S.A., Tounsi, A. and Mahmoud, S.R. (2017), "A new nonlocal trigonometric shear deformation theory for thermal buckling analysis of embedded nanosize FG plates", *Struct. Eng. Mech., Int. J.*, **64**(4), 391-402. https://doi.org/10.12989/sem.2017.64.4.391

Kolahchi, R., Bidgoli, M.R., Beygipoor, G. and Fakhar, M.H. (2015), "A nonlocal nonlinear analysis for buckling in embedded FG-SWCNT-reinforced microplates subjected to magnetic field", *J. Mech. Sci. Technol.*, **29**(9), 3669-3677. https://doi.org/10.1007/s12206-015-0811-9

Kováčik, J. (1999), "Correlation between Young's modulus and porosity in porous materials", *J. Mater. Sci. Lett.*, **18**(13), 1007-1010. https://doi.org/10.1023/A:1006669914946

Lakshmipathi, J. and Vasudevan, R. (2019), "Dynamic characterization of a CNT reinforced hybrid uniform and non-uniform composite plates", *Steel Compos. Struct., Int. J.*, **30**(1), 31-46. https://doi.org/10.12989/scs.2019.30.1.031

Lei, Z.X., Liew, K.M. and Yu, J.L. (2013), "Buckling analysis of functionally graded carbon nanotube reinforced composite plates using the element-free kp-Ritz method", *Compos. Struct.*, **98**, 160-168. https://doi.org/10.1016/j.compstruct.2012.11.006

Li, H., Tu, S., Liu, Y., Lu, X. and Zhu, X. (2019), "Mechanical Properties of L-joint with composite sandwich structure", *Compos. Struct.*, **217**, 165-174. https://doi.org/10.1016/j.compstruct.2019.03.011

Liu, L., Zhang, B.D., Wang, D.F. and Wu, Z.J. (2006), "Effects of cure cycles on void content and mechanical properties of composites laminates", *Compos. Struct.*, **73**(3), 303-309. https://doi.org/10.1016/j.compstruct.2005.02.001

Mahapatra, T.R., Mehar, K., Panda, S.K., Dewangan, S. and Dash, S. (2017), "Flexural strength of functionally graded nanotube reinforced sandwich spherical panel", *Proceedings of IOP conference series: Mater. Sci. Eng.*, Vol. 178, No. 1, p. 012031. https://doi.org/10.1088/1757-899X/178/1/012031

Mehar, K. and Panda, S.K. (2016a), "Free vibration and bending behaviour of CNT reinforced composite plate using different shear deformation theory", *Proceedings of IOP Conference Series: Mater. Sci. Eng.*, Vol. 115, No. 1, p. 012014. https://doi.org/10.1088/1757-899X/115/1/012014

Mehar, K. and Panda, S.K. (2016b), "Geometrical nonlinear free vibration analysis of FG-CNT reinforced composite flat panel under uniform thermal field", *Compos. Struct.*, **143**, 336-346. https://doi.org/10.1016/j.compstruct.2016.02.038

Mehar, K. and Panda, S.K. (2016c), "Nonlinear static behavior of FG-CNT reinforced composite flat panel under thermomechanical load", *J. Aerosp. Eng.*, **30**(3), 04016100. https://doi.org/10.1061/(ASCE)AS.1943-5525.0000706

Mehar, K. and Panda, S.K. (2017a), "Numerical investigation of nonlinear thermomechanical deflection of functionally graded CNT reinforced doubly curved composite shell panel under different mechanical loads", *Compos. Struct.*, **161**, 287-298. https://doi.org/10.1016/j.compstruct.2016.10.135

Mehar, K. and Panda, S.K. (2017b), "Thermoelastic analysis of FG-CNT reinforced shear deformable composite plate under various loadings", *Int. J. Computat. Methods*, **14**(2), 1750019. https://doi.org/10.1142/S0219876217500190

Mehar, K. and Panda, S.K. (2018a), "Thermal free vibration behavior of FG-CNT reinforced sandwich curved panel using finite element method", *Polym. Compos.*, **39**(8), 2751-2764. https://doi.org/10.1002/pc.24266

Mehar, K. and Panda, S.K. (2018b), "Dynamic response of functionally graded carbon nanotube reinforced sandwich plate", *Proceedings of IOP Conference Series: Mater. Sci. Eng.*, Vol. 338, No. 1, p. 012017. https://doi.org/10.1088/1757-899X/338/1/012017

Mehar, K. and Panda, S.K. (2018c), "Elastic bending and stress analysis of carbon nanotube-reinforced composite plate: Experimental, numerical, and simulation", *Adv. Polym. Technol.*, **37**(6), 1643-1657. https://doi.org/10.1002/adv.21821

Mehar, K. and Panda, S.K. (2018d), "Nonlinear finite element solutions of thermoelastic flexural strength and stress values of temperature dependent graded CNT-reinforced sandwich shallow shell structure", *Struct. Eng. Mech., Int. J.*, **67**(6), 565-578. https://doi.org/10.12989/sem.2018.67.6.565

Mehar, K. and Panda, S.K. (2018e), "Thermoelastic flexural analysis of FG-CNT doubly curved shell panel", *Aircraft Eng. Aerospace Technol.*, **90**(1), 11-23. https://doi.org/10.1108/AEAT-11-2015-0237

Mehar, K. and Panda, S.K. (2019), "Theoretical deflection analysis of multi-walled carbon nanotube reinforced sandwich panel and experimental verification", *Compos. Part B: Eng.*, **167**, 317-328. https://doi.org/10.1016/j.compositesb.2018.12.058

Mehar, K., Panda, S.K., Dehengia, A. and Kar, V.R. (2016), "Vibration analysis of functionally graded carbon nanotube reinforced composite plate in thermal environment", *J. Sandw. Struct. Mater.*, **18**(2), 151-173. https://doi.org/10.1016/j.compstruct.2019.03.002

Mehar, K., Panda, S.K., Bui, T.Q. and Mahapatra, T.R. (2017a), "Nonlinear thermoelastic frequency analysis of functionally graded CNT-reinforced single/doubly curved shallow shell panels by FEM", *J. Thermal Stress.*, **40**(7), 899-916. https://doi.org/10.1080/01495739.2017.1318689

Mehar, K., Panda, S.K. and Mahapatra, T.R. (2017b), "Theoretical and experimental investigation of vibration characteristic of carbon nanotube reinforced polymer composite structure", *Int. J. Mech. Sci.*, **133**, 319-329. https://doi.org/10.1016/j.ijmecsci.2017.08.057

Mehar, K., Panda, S.K. and Mahapatra, T.R. (2017c), "Thermoelastic nonlinear frequency analysis of CNT reinforced functionally graded sandwich structure", *Eur. J. Mech.-A/Solids*, **65**, 384-396. https://doi.org/10.1016/j.euromechsol.2017.05.005

Mehar, K., Panda, S.K. and Patle, B.K. (2017d), "Thermoelastic vibration and flexural behavior of FG-CNT reinforced composite curved panel", *Int. J. Appl. Mech.*, **9**(4), 1750046. https://doi.org/10.1142/S1758825117500466

Mehar, K., Mahapatra, T.R., Panda, S.K., Katariya, P.V. and Tompe, U.K. (2018a), "Finite-element solution to nonlocal elasticity and scale effect on frequency behavior of shear deformable nanoplate structure", *J. Eng. Mech.*, **144**(9), 04018094. https://doi.org/10.1061/(ASCE)EM.1943-7889.0001519

Mehar, K., Panda, S.K. and Mahapatra, T.R. (2018b), "Nonlinear frequency responses of functionally graded carbon nanotube-reinforced sandwich curved panel under uniform temperature field", *Int. J. Appl. Mech.*, **10**(3), 1850028. https://doi.org/10.1142/S175882511850028X

Mehar, K., Panda, S.K. and Mahapatra, T.R. (2018c), "Thermoelastic deflection responses of CNT reinforced sandwich shell structure using finite element method", *Scientia Iranica*, **25**(5), 2722-2737. https://doi.org/10.24200/SCI.2017.4525

Mehar, K., Panda, S.K. and Patle, B.K. (2018d), "Stress, deflection, and frequency analysis of CNT reinforced graded sandwich plate under uniform and linear thermal environment: A finite element approach", *Polym. Compos.*, **39**(10), 3792-3809. https://doi.org/10.1002/pc.24409

Mehar, K., Panda, S.K., Devarajan, Y. and Choubey, G. (2019a), "Numerical buckling analysis of graded CNT-reinforced composite sandwich shell structure under thermal loading", *Compos. Struct.*, **216**, 406-414. https://doi.org/10.1016/j.compstruct.2019.03.002

Mehar, K., Panda, S.K. and Mahapatra, T.R. (2019b), "Large deformation bending responses of nanotube-reinforced polymer composite panel structure: Numerical and experimental analyses", *Proceedings of the Institution of Mechanical Engineers, Part G: J. Aerosp. Eng.*, **233**(5), 1695-1704. https://doi.org/10.1177/0954410018761192

Meksi, R., Benyoucef, S., Mahmoudi, A., Tounsi, A., Adda Bedia, E.A. and Mahmoud, S.R. (2019), "An analytical solution for bending, buckling and vibration responses of FGM sandwich plates", *J. Sandw. Struct. Mater.*, **21**(2), 727-757. https://doi.org/10.1177/1099636217698443

Menasria, A., Bouhadra, A., Tounsi, A., Bousahla, A.A. and Mahmoud, S.R. (2017), "A new and simple HSDT for thermal stability analysis of FG sandwich plates", *Steel Compos. Struct., Int. J.*, **25**(2), 157-175. https://doi.org/10.12989/scs.2017.25.2.157

Mokhtar, Y., Heireche, H., Bousahla, A.A., Houari, M.S.A., Tounsi, A. and Mahmoud, S.R. (2018), "A novel shear deformation theory for buckling analysis of single layer graphene sheet based on nonlocal elasticity theory", *Smart Struct. Syst., Int. J.*, **21**(4), 397-405. https://doi.org/10.12989/sss.2018.21.4.397

Moradi-Dastjerdi, R. (2016), "Wave propagation in functionally graded composite cylinders reinforced by aggregated carbon nanotube", *Struct. Eng. Mech., Int. J.*, **57**(3), 441-456. https://doi.org/10.12989/sem.2016.57.3.441

Mouffoki, A., Adda Bedia, E.A., Houari, M.S.A., Tounsi, A. and Mahmoud, S.R. (2017), "Vibration analysis of nonlocal advanced nanobeams in hygro-thermal environment using a new two-unknown trigonometric shear deformation beam theory", *Smart Struct. Syst., Int. J.*, **20**(3), 369-383. https://doi.org/10.12989/sss.2017.20.3.369

Muller, E., Drasar, C., Schilz, J. and Kaysser, W.A. (2003), "Functionally graded materials for sensor and energy applications", *Mater. Sci. Eng. A*, **362**(1-2), 17-39. https://doi.org/10.1016/S0921-5093(03)00581-1

Panda, K.C., Bhattacharyya, S.K. and Barai, S.V. (2012), "Shear behaviour of RC T-beams strengthened with U-wrapped GFRP sheet", *Steel Compos. Struct., Int. J.*, **12**(2), 149-166. https://doi.org/10.12989/scs.2012.12.2.149

Rakrak, K., Zidour, M., Heireche, H., Bousahla, A.A. and Chemi, A. (2016), "Free vibration analysis of chiral double-walled carbon nanotube using non-local elasticity theory", *Adv. Nano Res., Int. J.*, **4**(1), 31-44. https://doi.org/10.12989/anr.2016.4.1.031

Reddy, J.N. (2004), *Mechanics of Laminated Composite Plates and Shells: Theory and Analysis*, (2nd Edition), Taylor & Francis eBooks, CRC Press.

Rezaiee-Pajand, M., Sani, A.A. and Hozhabrossadati, S.M. (2019), "Deflection of axially functionally graded rectangular plates by Green's function method", *Steel Compos. Struct., Int. J.*, **30**(1), 57-67. https://doi.org/10.12989/scs.2019.30.1.057

Safaei, B., Moradi-Dastjerdi, R., Qin, Z. and Chu, F. (2019), "Frequency-dependent forced vibration analysis of nanocomposite sandwich plate under thermo-mechanical loads", *Composites Part B: Eng.*, **161**, 44-54. https://doi.org/10.1016/j.compositesb.2018.10.049

Sahmani, S., Aghdam, M.M. and Rabczuk, T. (2018), "A unified nonlocal strain gradient plate model for nonlinear axial instability of functionally graded porous micro/nano-plates reinforced with graphene platelets", *Mater. Res. Express*, **5**(4), 045048. https://doi.org/10.1088/2053-1591/aabdbb

Semmah, A., Heireche, H., Bousahla, A.A. and Tounsi, A. (2019), "Thermal buckling analysis of SWBNNT on Winkler foundation by non local FSDT", *Adv. Nano Res., Int. J.*, **7**(2), 89-98. https://doi.org/10.12989/anr.2019.7.2.089

Shafiei, H. and Setoodeh, A.R. (2017), "Nonlinear free vibration and post-buckling of FG-CNTRC beams on nonlinear foundation", *Steel Compos. Struct., Int. J.*, **24**(1), 65-77. https://doi.org/10.12989/scs.2017.24.1.065

Shahsavari, D., Karami, B. and Li, L. (2018), "A high-order gradient model for wave propagation analysis of porous FG nanoplates", *Steel Compos. Struct., Int. J.*, **29**(1), 53-66. https://doi.org/10.12989/scs.2018.29.1.053

Sharma, N., Mahapatra, T.R., Panda, S.K. and Mehar, K. (2018), "Evaluation of vibroacoustic responses of laminated composite sandwich structure using higher-order finite-boundary element model", *Steel Compos. Struct., Int. J.*, **28**(5), 629-639. https://doi.org/10.12989/scs.2018.28.5.629

Shokravi, M. (2017), "Buckling of sandwich plates with FG-CNT-reinforced layers resting on orthotropic elastic medium using Reddy plate theory", *Steel Compos. Struct., Int. J.*, **23**(6), 623-631. https://doi.org/10.12989/scs.2017.23.6.623

Shu, D. and Fan, H. (1996), "Free vibration of a bimaterial split beam", *Compos. Part B*, **27**(1), 79-84. https://doi.org/10.1016/1359-8368(95)00026-7

Tlidji, Y., Zidour, M., Draiche, K., Safa, A., Bourada, M., Tounsi, A., Bousahla, A.A. and Mahmoud, S.R. (2019), "Vibration analysis of different material distributions of functionally graded microbeam", *Struct. Eng. Mech., Int. J.*, **69**(6), 637-649. https://doi.org/10.12989/sem.2019.69.6.637

Wattanasakulpong, N. and Chaikittiratana, A. (2015), "Exact solutions for static and dynamic analyses of carbon nanotube-reinforced composite plates with Pasternak elastic foundation", *Appl. Math. Model.*, **39**(18), 5459-5472. https://doi.org/10.1016/j.apm.2014.12.058

Xiao, W., Yan, C., Tian, W., Tian, W. and Song, X. (2018), "Effects of face-sheet materials on the flexural behavior of aluminum foam sandwich", *Steel Compos. Struct., Int. J.*, **29**(3), 301-308. https://doi.org/10.12989/scs.2018.29.3.301

Yazid, M., Heireche, H., Tounsi, A., Bousahla, A.A. and Houari, M.S.A. (2018), "A novel nonlocal refined plate theory for stability response of orthotropic single-layer graphene sheet resting on elastic medium", *Smart Struct. Syst., Int. J.*, **21**(1), 15-25. https://doi.org/10.12989/sss.2018.21.1.015

Youcef, D.O., Kaci, A., Benzair, A., Bousahla, A.A. and Tounsi, A. (2018), "Dynamic analysis of nanoscale beams including surface stress effects", *Smart Struct. Syst., Int. J.*, **21**(1), 65-74. https://doi.org/10.12989/sss.2018.21.1.065

Younsi, A., Tounsi, A, Zaoui, F.Z., Bousahla, A.A. and Mahmoud, S.R. (2018), "Novel quasi-3D and 2D shear deformation theories for bending and free vibration analysis of FGM plates", *Geomech. Eng., Int. J.*, **14**(6), 519-532. https://doi.org/10.12989/gae.2018.14.6.519

Zaoui, F.Z., Ouinas, D. and Tounsi, A. (2019), "New 2D and quasi-3D shear deformation theories for free vibration of functionally graded plates on elastic foundations", *Compos. Part B*, **159**, 231-247. https://doi.org/10.1016/j.compositesb.2018.09.051

Zarga, D., Tounsi, A., Bousahla, A.A., Bourada, F. and Mahmoud, S.R. (2019), "Thermomechanical bending study for functionally graded sandwich plates using a simple quasi-3D shear deformation theory", *Steel Compos. Struct., Int. J.*, **32**(3), 389-410. https://doi.org/10.12989/scs.2019.32.3.389

Zemri, A., Houari, M.S.A., Bousahla, A.A. and Tounsi, A. (2015), "A mechanical response of functionally graded nanoscale beam: an assessment of a refined nonlocal shear deformation theory beam theory", *Struct. Eng. Mech., Int. J.*, **54**(4), 693-710. https://doi.org/10.12989/sem.2015.54.4.693

Zhu, P., Lei, Z.X. and Liew, K.M. (2012), "Static and free vibration analyses of carbon nanotube reinforced composite plates using finite element method with first order shear deformation plate theory", *Compos. Struct.*, **94**, 1450-1460. https://doi.org/10.1016/j.compstruct.2011.11.010

Zidour, M., Hadji, L., Bouazza, M., Tounsi, A. and Bedia, E.A. (2015), "The mechanical properties of Zigzag carbon nanotube using the energy-equivalent model", *J. Chem. Mater. Res.*, **3**, 9-14.

Zine, A., Tounsi, A., Draiche, K., Sekkal, M. and Mahmoud, S.R. (2018), "A novel higher-order shear deformation theory for bending and free vibration analysis of isotropic and multilayered plates and shells", *Steel Compos. Struct., Int. J.*, **26**(2), 125-137. https://doi.org/10.12989/scs.2018.26.2.125

CC